Simplified Evaluation Methods for Impedance and Foundation Input Motion of Embedded Foundation

M. Mori, N. Fukuwa & J. Tobita
Nagoya University, Nagoya, Japan

T. Suzuki
Takenaka Corporation, Tokyo, Japan

SUMMARY:
In this paper, we propose conventional evaluation methods of impedances and foundation input motions for the dynamic soil-structure interaction analysis of buildings with embedment foundations. Two simplified methods of foundation input motion are shown. One is the least squares method based on the geometrical relationship between each part of the foundation; side elements and a bottom element, and ground motions. The other one is the weighted average method. The weighted average method uses the driving force and the impedance of the embedded foundation. Here, we proposed a new conventional method for evaluating the impedance of embedded foundation. In this method, the impedance of the embedded foundation is evaluated by extending our proposed method (Mori *et al.*, 2008). The validity of the proposed methods is shown by comparing the results with those obtained from an existing numerical method through parametric analyses.

Keywords: Dynamic Soil-Structure Interaction, Impedance, Foundation Input Motion

1. INTRODUCTION

It is very important to consider the dynamic soil-structure interaction (SSI) when we study on the behaviour of buildings with embedded foundation or pile foundation under strong ground motion. Evaluating the effect of the SSI on the dynamic response of buildings appropriately, an impedance of the foundation and the foundation input motion are needed. However, unfortunately, it is difficult for structure designers to evaluate the basic physical values of the SSI by using the theoretical method. Therefore, simplified evaluation methods of impedances and foundation input motions are necessary, especially for embedment foundations. Iguchi (1982), Kurimoto and Iguchi (1995) , Kurimoto and Seki (1995), etc. reported about the conventional estimation methods for the foundation input motion of the embedded foundation.

In this paper, we propose simplified evaluation methods for impedance and foundation input motion of embedded foundation. The estimation method developed by WEN and Fukuwa (2006) are applied to this examination. First of all, we propose conventional evaluation methods of foundation input motions for the dynamic soil-structure interaction analysis of buildings with embedment foundations. Two simplified methods are shown. One is the least squares method based on the geometrical relationship between each part of the foundation; side elements and a bottom element, and ground motions. The other one is the weighted average method. The weighted average method uses the driving force and the impedance of the embedded foundation. Here, we proposed a new conventional method for evaluating the impedance of embedded foundation. In this method, the impedance is evaluated by extending our already proposed method (Mori *et al.*, 2008). The impedance is calculated as the summation of impedances both of every side elements and bottom element of the embedded foundation. The modified impedance of the spread foundation by the compensation factors proposed by Sugimoto *et al.* (2010) is applied for evaluating these impedances. But these factors don't have the clear physical meaning. Therefore, we modify these factors in order to explain the physical meaning of the compensation factor in this study.

The accuracy and validity of the proposed methods are shown by comparing the results with those obtained from an existing numerical method through parametric analyses.

2. SIMPLIFIED METHODS FOR FOUNDATION INPUT MOTION OF EMBEDDED FOUNDATION

We propose two simplified methods for foundation input motion of embedded foundation. One is the least squares method based on the geometrical relationship between each part of the foundation and ground motion. The other method is the weighted average method which uses the simplified evaluation for the driving force and the impedance of the embedded foundation. This impedance is derived from the modified impedance of the spread foundation by applying proposed compensation factors. The driving force is obtained by multiplying the modified impedance and the ground motion. In this section, these two evaluation methods are explained briefly.

2.1. The Least Squares Method (Simple Analytical Solution I: Method I)

This is the extension method of the approximate solution of foundation input motions for spread foundations (AIJ, 1996). Namely, the foundation input motion is evaluated under the condition that the relative displacement between the foundation and the ground motion becomes the minimum when the harmonic ground motion enters into the assumed rigid foundation on the homogeneous half space soil. The solution can be obtained simply by using the shape of foundation, the shear velocity of the soil and the incident angle of the input motion because the geometrical relationship between the foundation and the ground motion is just considered. The schematic model in this study is shown in Fig. 2.1. The foundation is assumed to be rigid and square. The size and the embedded depth of the foundation is assumed to be $2b\times 2c$ and E, respectively. The input motion is the harmonic vibration and its components are presented $(u,v,w)e^{iwt}$, where u, v and w are found in Fig.2.1. For simplicity, the time factor e^{iwt} is eliminated. The foundation input motion of the embedded foundation is evaluated at the centroid of the foundation. An origin of coordinates is set to this point. The input motion has a six degree of freedom expressed as follows.

$$\{U^*\} = \left\{\varDelta_x^*\ ,\varDelta_y^*\ ,\varDelta_z^*\ ,\varPhi_x^*\ ,\varPhi_y^*\ ,\varPhi_z^*\right\}^T \tag{2.1}$$

Here, $\varDelta_x^*$, $\varDelta_y^*$ and $\varDelta_z^*$ is the translational displacement in each direction, $\varPhi_x^*$, $\varPhi_y^*$ and $\varPhi_z^*$ is the rotation in each direction at the centre of the foundation.

First of all, the bottom element and the side elements are decomposed from the embedment foundation. The square sum of the relative displacements between these elements and the ground motion is defined as follows.

$$W = \sum\int\left\{\left(\Delta_x^* - y\Phi_z^* + z\Phi_y^*\right) - u\right\}^2 dS_i + \sum\int\left\{\left(\Delta_y^* + x\Phi_z^* - z\Phi_x^*\right) - v\right\}^2 dS_i + \sum\int\left\{\left(\Delta_z^* + y\Phi_x^* - x\Phi_y^*\right) - w\right\}^2 dS_i \tag{2.2}$$

Here, S_i is the area of each element. The input motion is obtained by setting the partial differential about each component of Eqn. 2.2 to zero shown as follows.

$$\Delta_x^* = \frac{C_0}{A}\sum\int u dS_i - C_1 E\Phi_y^* \tag{2.3}$$

$$\Delta_y^* = \frac{C_0}{A}\sum\int v dS_i + C_1 E\Phi_x^* \tag{2.4}$$

$$\Delta_z^* = \frac{C_0}{A}\sum\int w dS_i \tag{2.5}$$

z

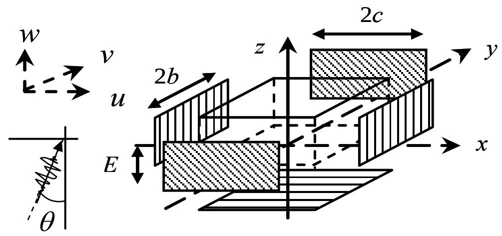

Figure 2.1 Embedded foundation and the coordinate system

$$\Phi_x^* = \frac{C_2}{I_x}\sum\int\{yw-(z-C_1E)v\}dS_i \tag{2.6}$$

$$\Phi_y^* = \frac{C_3}{I_y}\sum\int\{(z-C_1E)u-xw\}dS_i \tag{2.7}$$

$$\Phi_z^* = \frac{C_4}{I_x+I_y}\sum\int(xv-yu)dS_i \tag{2.8}$$

Here, C_0 is the ratio of the area A of the bottom to the total surface area of the foundation, C_1 is the coefficient presenting the centre of the figure in the direction of the depth, and C_2, C_3 and C_4 are the ratios of geometrical moment of inertia I_x, I_y, and I_x+I_y to the sum of I_x, I_y, and I_x+I_y at all decomposed foundation elements. These coefficients are shown in Eqn. 2.9 to Eqn. 2.13.

$$C_0 = A\Big/\sum\int dS_i \tag{2.9}$$

$$C_1 = \frac{1}{E}\times\sum\int zdS_i\Big/\sum\int dS_i \tag{2.10}$$

$$C_2 = I_x\Big/\left\{\sum\int(y^2+z^2)dS_i-\left(\sum\int zdS_i\right)^2\Big/\sum\int dS_i\right\} \tag{2.11}$$

$$C_3 = I_y\Big/\left\{\sum\int(x^2+z^2)dS_i-\left(\sum\int zdS_i\right)^2\Big/\sum\int dS_i\right\} \tag{2.12}$$

$$C_4 = (I_x+I_y)\Big/\sum\int(x^2+y^2)dS_i \tag{2.13}$$

The estimation equations for the foundation input motion are applied to some concrete problems. When SH wave in the x direction incidents perpendicularly or obliquely to the embedded foundation as shown in Fig. 2.1, the foundation input motion is estimated by using the estimation equations above mentioned. When the displacement of the ground motion at the soil surface is U_0, the incident angle of SH wave is θ and the shear velocity of the soil is V_s, the full-field displacement of the ground motion is presented as follows.

$$u(y,z) = U_0\cos\left\{\frac{\omega\cos\theta}{Vs}(z-E)\right\}\exp\left(-i\frac{\omega\sin\theta}{Vs}y\right) \tag{2.14}$$

In the case of the perpendicular incidence, the incident angle θ is set to zero in Eqn. 2.14. The foundation input motion can be expressed as follows by substituting Eqn. 2.14 for Eqn. 2.8 from Eqn. 2.3.

$$\begin{aligned}\Delta_x^* = U_0C_0\{&\cos(E/b_e\cdot a_0)\\ &+E/b_e\cdot\left(\sqrt{c/b}+\frac{1}{\sqrt{c/b}}\right)j_0(E/b_e\cdot a_0)\Big\}-C_1E\Phi_y^*\end{aligned} \tag{2.15}$$

$$\begin{aligned}\Phi_y^*\times b_e = U_0\frac{3C_3(E/b_e)^2}{c/b}&\left[\left(\sqrt{c/b}+\frac{1}{\sqrt{c/b}}\right)\frac{1-\cos(E/b_e\cdot a_0)}{(E/b_e\cdot a_0)^2}\right.\\ &\left.-C_1\left\{\frac{1}{E/b_e}\cos(E/b_e\cdot a_0)+\left(\sqrt{c/b}+\frac{1}{\sqrt{c/b}}\right)j_0(E/b_e\cdot a_0)\right\}\right]\end{aligned} \tag{2.16}$$

In the case of the oblique incidence of SH wave, the foundation input motion is expressed as follows.

$$\begin{aligned}\Delta_x^* &= U_0 C_0 \left[j_0\left(\frac{1}{\sqrt{c/b}} a_0 \sin\theta\right)\cos\left(E/b_e \cdot a_0 \cos\theta\right)\right.\\ &+ E/b_e \cdot \left\{\sqrt{c/b}\cos\left(\frac{1}{\sqrt{c/b}} a_0 \sin\theta\right) + \frac{1}{\sqrt{c/b}} j_0\left(\frac{1}{\sqrt{c/b}} a_0 \sin\theta\right)\right\}\\ &\left.\times j_0\left(E/b_e \cdot a_0 \cos\theta\right)\right] - C_1 E \Phi_y^*\end{aligned} \tag{2.17}$$

$$\begin{aligned}\Phi_y^* \times b_e &= U_0 \frac{3C_3 (E/b_e)^2}{c/b}\left[\left\{\sqrt{c/b}\cos\left(\frac{1}{\sqrt{c/b}} a_0 \sin\theta\right) + \frac{1}{\sqrt{c/b}} j_0\left(\frac{1}{\sqrt{c/b}} a_0 \sin\theta\right)\right\}\right.\\ &\times \frac{1-\cos\left(E/b_e \cdot a_0 \cos\theta\right)}{\left(E/b_e \cdot a_0 \cos\theta\right)^2} - \frac{C_1}{E/b_e} j_0\left(\frac{1}{\sqrt{c/b}} a_0 \sin\theta\right)\cos\left(E/b_e \cdot a_0 \cos\theta\right)\\ &\left.- C_1\left\{\sqrt{c/b}\cos\left(\frac{1}{\sqrt{c/b}} a_0 \sin\theta\right) + \frac{1}{\sqrt{c/b}} j_0\left(\frac{1}{\sqrt{c/b}} a_0 \sin\theta\right)\right\} j_0\left(E/b_e \cdot a_0 \cos\theta\right)\right]\end{aligned} \tag{2.18}$$

$$\begin{aligned}\Phi_z^* \times b_e &= iU_0 \frac{3C_4\sqrt{c/b}}{1+(c/b)^2}\left[j_1\left(\frac{1}{\sqrt{c/b}} a_0 \sin\theta\right)\cos\left(E/b_e \cdot a_0 \cos\theta\right)\right.\\ &+ E/b_e \cdot \left\{\sqrt{c/b}\sin\left(\frac{1}{\sqrt{c/b}} a_0 \sin\theta\right) + \frac{1}{\sqrt{c/b}} j_1\left(\frac{1}{\sqrt{c/b}} a_0 \sin\theta\right)\right\}\\ &\left.\times j_0\left(E/b_e \cdot a_0 \cos\theta\right)\right]\end{aligned} \tag{2.19}$$

Here, b_e is the width of a square foundation whose area is equivalent to the bottom area of the foundation, a_0 is the non-dimensional frequency; $a_0=\omega b_e/V_s$, and $j_0(\cdot)$ and $j_1(\cdot)$ are spherical Bessel functions shown as follows.

$$j_0(z) = \frac{\sin z}{z} \tag{2.20}$$

$$j_1(z) = \frac{\sin z}{z^2} - \frac{\cos z}{z} \tag{2.21}$$

2.2. The Weighted Average Method (Simple Analytical Solution II: Method II)

When the components of the driving force are F_H, F_R, the foundation input motion is expressed as follows by using the impedance of each component; K_{HH} for horizontal, K_{RR} for rotation and K_{HR}=K_{RH} for coupling between horizontal and rotation.

$$\begin{Bmatrix}\Delta_x^* \\ \Phi_y^*\end{Bmatrix} = \begin{bmatrix}K_{HH} & K_{HR} \\ K_{RH} & K_{RR}\end{bmatrix}^{-1}\begin{Bmatrix}F_H \\ F_R\end{Bmatrix} \tag{2.22}$$

The foundation input motion is calculated by using Eqn. 2.22 with the driving force and the impedance evaluated by a simple method which is introduced in the next division. In this study, the analysis condition is that the non-dimensional frequency a_0 is smaller than 3.0, the embedded depth ratio E/b_e is smaller than 1.0, and the aspect ratio c/b is larger than 0.1 and smaller than 10.0.

2.2.1. Simple evaluation of impedance

The impedance of an embedded foundation is evaluated simply by extending our past proposed method (Mori *et al*., 2008 and Sugimoto *et al*., 2010). According to this proposed method, the impedance of the embedded foundation is calculated as the summation of impedance of each element (side element and bottom element) of the embedded foundation by using two compensation factors α and γ. The compensation factor α considers the overlap of the soil which is included in the impedances of two adjacent elements of the embedded foundation (Mori *et al*., 2008). On the other hand, the compensation factor γ modifies the impedance due to the difference of the shape of each element on condition that the impedance of the square spread foundation on the same soil as the embedded foundation is known (Sugimoto *et al*., 2010). But the factor α doesn't have the clear physical meaning in their study. Therefore, we modify the factor α in order to explain its physical meaning.

The convenient evaluation method of the impedance is shown as Eqns. 2.23 to 2.26. The schematic figure of each side element of the embedded foundation is depicted in Fig. 2.2.

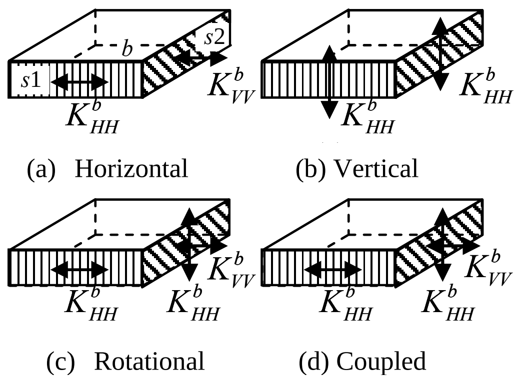

Figure 2.2 The summation of the impedance of each side element of the embedded foundation

$$K_{HH} = {}^{b}\gamma_1 K^b_{HH} + 2\alpha_{HH}\left({}^{s1}\gamma_1 K^b_{HH} + {}^{s2}\gamma_3 K^b_{VV}\right) \tag{2.23}$$

$$K_{VV} = {}^{b}\gamma_3 K^b_{VV} + 2\alpha_{VV}\left({}^{s1}\gamma_2 + {}^{s2}\gamma_2\right)K^b_{HH} \tag{2.24}$$

$$K_{RR} = {}^{b}\gamma_5 K^b_{RR} + 2\alpha_{RR}\left\{\left({}^{s1}\gamma_1 K^b_{HH} + {}^{s2}\gamma_3 K^b_{VV}\right)\times\left(\frac{E}{2}\right)^2 + {}^{s2}\gamma_2 K^b_{HH} c^2\right\} \tag{2.25}$$

$$K_{HR} = 2\alpha_{HH}\left({}^{s1}\gamma_1 K^b_{HH} + {}^{s2}\gamma_3 K^b_{VV}\right)\frac{E}{2} + 2\alpha_{VV}\,{}^{s2}\gamma_2 K^b_{HH} c \tag{2.26}$$

Here, K^b_{HH}, K^b_{VV} and K^b_{RR} are the horizontal impedance, the vertical impedance and the rotational impedance of the spread foundation, respectively. The subscription of α indicates each component of the impedance. γ is the shape modification factor of the impedance of the spread foundation proposed by Sugimoto *et al.* (2010) shown in Table 2.1. The schematic figure of their method is depicted in Fig. 2.3. In their method, γ is defined as the factor which presents the relationship between the foundation shape and the impedance. In Table 2.1, η is the ratio about the equivalent width to a square, λ is the aspect ratio of the bottom shape of the foundation as shown in Fig. 2.3. Right subscripts of γ in Eqns. 2.23 to 2.26 are the components of the impedance shown in Table 2.1. Left superscripts of γ in Eqns. 2.23 to 2.26 are kinds of surface of the embedded foundation depicted in Fig. 2.2. Namely, *b*, *s*1 and *s*2 indicate the bottom, the side surface parallel to the exciting direction and the side surface vertical to the exciting direction, respectively. And η and λ are calculated according to the shape of each surface above mentioned. For example, when the dimensions of an embedded foundation are assumed to be 2*b* x 2*c* x *E* as shown in Fig. 2.1, the correction factor ${}^{s1}\gamma_1$ in Eqns. 2.23 to 2.26 of the side surface, whose dimensions are E x 2*c*, is calculated by using $\eta = \sqrt{2cE/4bc}$, $\lambda = E/2c$. This process allows the factor α to correct purely the overlap of the soil which is included in the impedances of two adjacent surfaces of the embedment foundation.

Table 2.1 Compensation factors of the impedance

K_{11}	$\gamma_1 = \eta\times\left(0.55\lambda^{0.37} + 0.45\lambda^{-0.31}\right)$	$\gamma_1 = \eta^2$
K_{22}	$\gamma_2 = \eta\times\left(0.48\lambda^{0.28} + 0.52\lambda^{-0.38}\right)$	$\gamma_2 = \eta^2$
K_{33}	$\gamma_3 = \eta\times\left\{0.205\left(\sqrt{\lambda} + 1/\sqrt{\lambda}\right) + 0.59\right\}$	$\gamma_3 = \eta^2$
K_{44}	$\gamma_4 = \eta^3\times\lambda^{0.61}$	$\gamma_4 = \eta^{4.35}\times\lambda^{1.06}$
K_{55}	$\gamma_5 = \eta^3\times\lambda^{-0.86}$	$\gamma_5 = \eta^{4.35}\times\lambda^{-1.05}$
K_{66}	$\gamma_6 = \eta^3\times 0.49\left(\lambda + 1/\lambda\right)$	$\gamma_6 = \eta^{4.3}\times 0.66\lambda^{-0.9}\ (\lambda < 0.6)$ $\gamma_6 = 1.0\quad(\lambda \geq 0.6)$

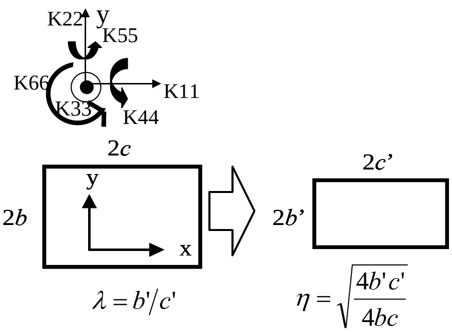

Figure 2.3 The schematic diagram of the shape modification

The factor α is estimated by the least-squares method in order to get good agreement with the theoretical solution. Then, it is presented as the function of E/b_e, which is the ratio of the depth to the equivalent width mentioned in subsection 2.1. As to the real part of the impedance, the estimation results are presented in Fig. 2.4. It is shown that α of each component increases in proportion to E/b_e, and that α_{HH}, α_{VV}, α_{RR} are good agreement with the theoretical solutions which are presented as (Fit.) . Here, the real part of K_{HR} in Eqn. 2.26 is supposed to be a function of α_{HH} and α_{VV} because they can estimate K_{HR} sufficiently.

In the other hand, the factor for the imaginary part of the impedance is set to 1.0. The reason is that the simple sum of the impedance of the side element and that of the bottom element does not overestimate the imaginary part of the impedance of the embedded foundation, because it depends on the ground contact area of each element. However, the coefficient of K_{HR} is set to 0.5 which has good correspondence with the theoretical solution under the condition that E/b_e is below 1.0 because the simple sum overestimates the impedance. The factor α is summarized in Table 2.2.

2.2.2. Simple evaluation of driving force

The schematic figure for estimation of the driving force is shown in Fig. 2.5. In Fig. 2.5, K^s_{HH} means the horizontal impedance of the side element and corresponds to the second term in Eqn. 2.23. The driving force is estimated by using the input motion under the excavated ground based on Excavation-based Dynamic Substructure Method. The embedded foundation is broken into side elements and bottom element in a similar way of the impedance as mentioned in division 2.2.1. The driving force F_H and F_R are calculated as shown in Eqn. 2.27 and Eqn. 2.28, respectively.

$$F_H = {}^b\gamma_1 K^b_{HH} \times u^b + 2\alpha_{HH}\left({}^{s1}\gamma_1 K^b_{HH} + {}^{s2}\gamma_3 K^b_{VV}\right) \times u^s - P_H \tag{2.27}$$

$$F_R = K_{HR} \times u^s \tag{2.28}$$

Here, u^b is the ground displacement at the bottom of the foundation. It is expressed as Eqn. 2.29 in the case of the perpendicular incidence of SH wave. u^s is the averaged ground displacement at the side of the foundation as shown in Eqn. 2.30. P_H is the excavation force at the bottom of the foundation. It is calculated as Eqn. 2.31 when the shear modulus of the soil is G.

$$u^b = U_0 \cos\left(E/b_e \cdot a_0\right) \tag{2.29}$$

$$u^s = U_0 j_0\left(E/b_e \cdot a_0\right) \tag{2.30}$$

$$P_H = 4U_0 G b_e a_0 \sin\left(E/b_e \cdot a_0\right) \tag{2.31}$$

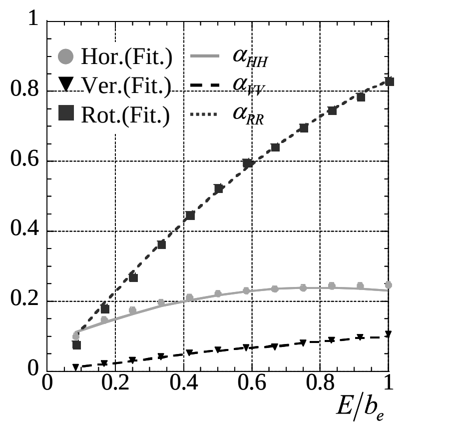

Figure 2.4 Comparison of the compensation factors α between proposed formula and theoretical solutions

Table 2.2 Compensation factor α in each component

	Re.	Imag.
α_{HH} (Hor.)	$-0.25\times(E/b_e)^2 + 0.4\times E/b_e + 0.08$	1.0
α_{VV} (Ver.)	$-0.03\times(E/b_e)^2 + 0.13\times E/b_e$	1.0
α_{RR} (Rot.)	$-0.4\times(E/b_e)^2 + 1.23\times E/b_e$	1.0
Coupling	α_{HH}、α_{VV} are applied	0.5

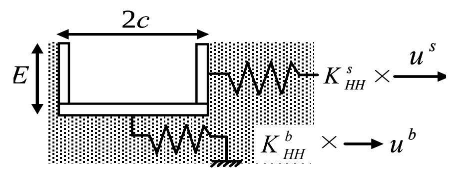

Figure 2.5 The schematic diagram of driving force

3. COMPARISON OF SIMPLIFIED EVALUATION RESULTS WITH EXACT SOLUTIONS

The analysis condition of the theoretical solution based on both Thin Layer Method and the Finite Element Method proposed by Wen *et al.* (2006) is mentioned at first. The size of the foundation and the soil profile are shown in Table 3.1 and Table 3.2, respectively. The embedded part of the foundation is translated into the solid hexahedron elements. The element mesh size is 1(m) x 1(m) x E/4(m). The impedance of the spread foundation applied to Method II (in subsection 2.2) is presented in Fig. 3.1.

The vertical axes in Figs.3.1 to 3.3 are non-dimensional impedances K_{HH}/Gb_e, K_{VV}/Gb_e, K_{RR}/Gb_e^3. The vertical axes in Figs.6 to 8 are transfer functions of the displacement at the foundation to U_0 at the ground surface; Δ_x^*/U_0, $\Phi_y^* b_e/U_0$, $\Phi_z^* b_e/U_0$. The horizontal axis in Figs.3.1 to 3.8 is the non-dimensional frequency a_0. In these figures, 'Sol.' means the theoretical solution.

In the case of Method II, the impedance in Eqns. 2.23 to 2.26 and the driving force in Eqns. 2.27 and 2.28 are used. Then, the validity of this method is performed by comparing the results with the theoretical solutions, at first. The results are shown in Fig. 3.2, where the ratio of the buried depth to the equivalent width E/b_e is set as a parameter. The results, where the aspect ratio of the plane shape of the foundation c/b is set as a parameter, are shown in Fig, 3.3. From these figures, it is recognized that the results have good agreement with the theoretical solutions comparatively, except for the decreasing tendency of the real part of (a) horizontal and (d) horizontal-rotation coupling component in the high frequency domain where the impedance is affected by the additional mass. It is found that the aspect ratio effects on the results of (a), (d) in the high frequency domain and (c), and that the effect of the additional mass is larger in accordance with decreasing aspect ratio. The reason is considered that γ is estimated based on the quasi-static solution. Therefore, the applicable range of the aspect ratio c/b is set from 0.5 to 2.0, where the impedance by using the proposed method is good agreement with the theoretical solution.

The comparison of the driving force estimated by the proposed method with that calculated by the theoretical method is shown in Figs. 3.4 and 3.5. As for Fig. 3.4, the ratio of the buried depth to the equivalent foundation width E/b_e is set as a parameter. As for Fig. 3.5, the aspect ratio of the plane shape of the foundation c/b is set as a parameter. The theoretical solution is applied to the estimation of the driving force in order to verify the validity of the Eqns. 2.27 and 2.28. The driving force of (a) horizontal component in Figs. 3.4 and 3.5 is good correspondence with the theoretical solution. As for (b) rotation components in Figs. 3.4 and 3.5, it is found that these are good

Table 3.1 Shape of foundation

	case-1	case-2	case-3	case-4
$2b$ (m)	24	24	30	18
$2c$ (m)	24	24	19.2	32
E (m)	4	12	12	12
c/b	1.00	1.00	0.64	1.78
E/b_e	0.33	1.00	1.00	1.00

Table 3.2 Soil profile

Vs (m/s)	ρ (t/m³)	ν	h
250	1.8	0.45	0.03

(Half-space soil)

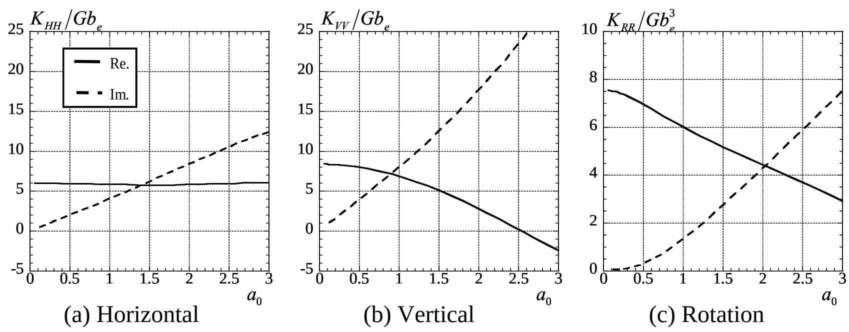

(a) Horizontal (b) Vertical (c) Rotation

Figure 3.1 Impedance of the spread foundation treated in this study

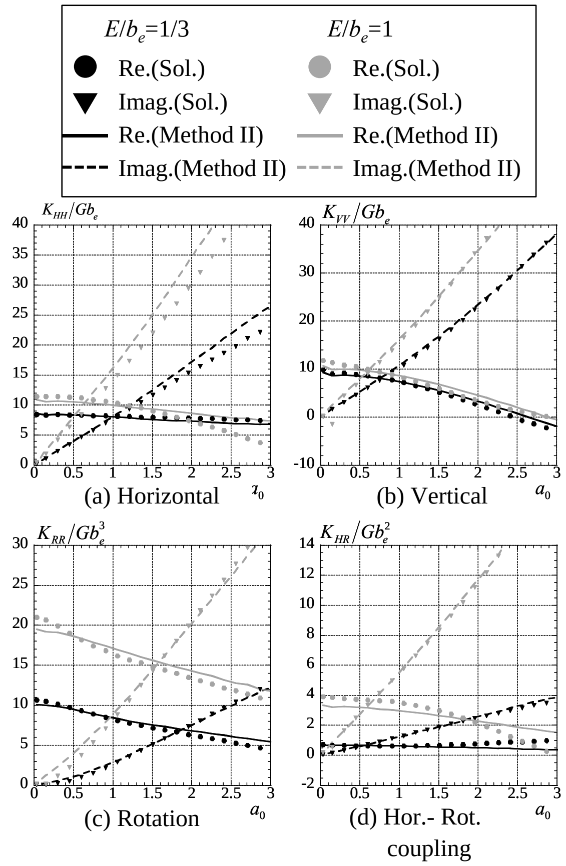

Figure 3.2 Comparison of the impedance using Method II (E/b_e is set as a parameter. c/b=1)

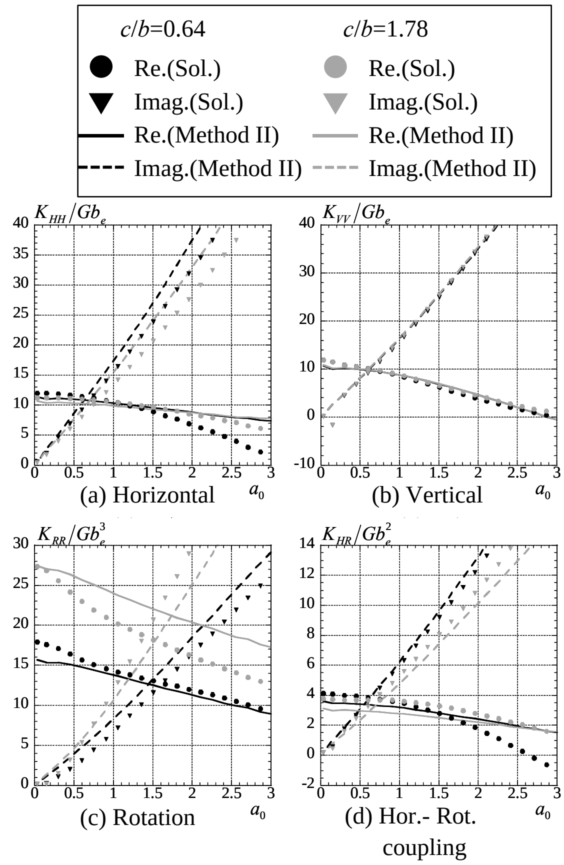

Figure 3.3 Comparison of the impedance using Method II (c/b is set as a parameter. E/b_e =1)

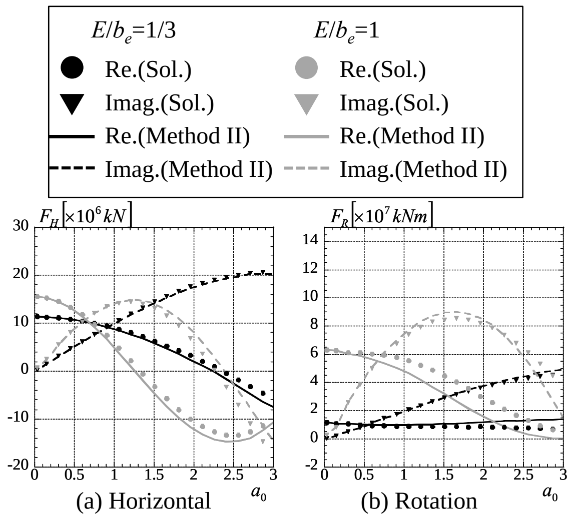

Figure 3.4 Comparison of the driving force (E/b_e is set as a parameter. c/b=1)

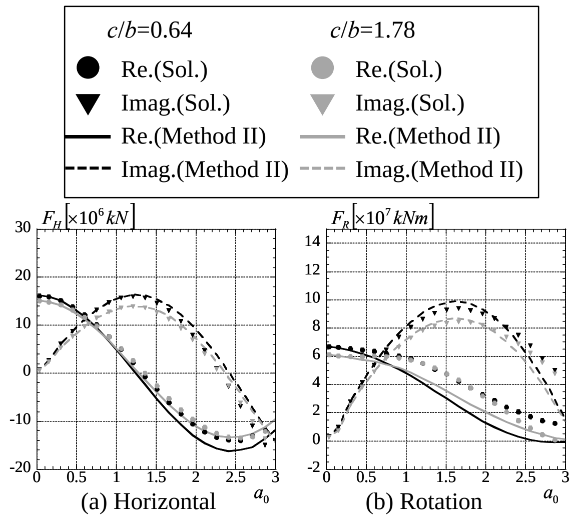

Figure 3.5 Comparison of the driving force (c/b is set as a parameter. E/b_e=1)

agreement with the theoretical solution under the quasi-static condition. However, the correspondence between these values is not so good, when E/b_e is larger than 1.0. Two reasons why the rotational impedance is not good correspondence according to the larger ratio E/b_e are considered. One is that the impedance of the side element is estimated only at the centre of the element in Eqn. 2.28. The other is that the ground displacement at the point is simply averaged along by the depth of the foundation. Therefore, the applicable range of E/b_e is set below 1.0. On the other hand, it is recognized in Fig. 3.5 that the effect of the aspect ratio c/b on Method II is very small.

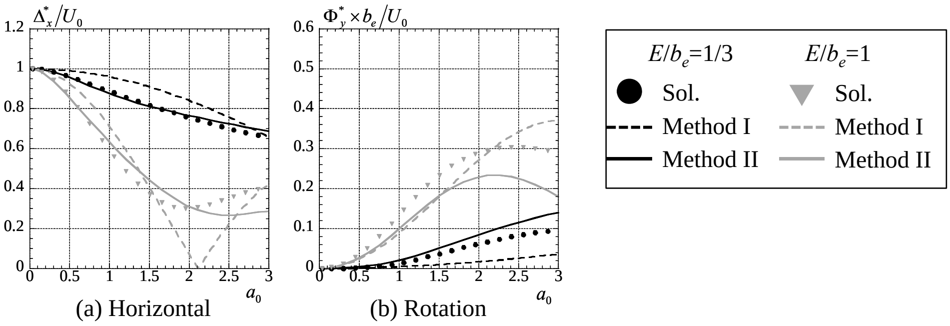

Figure 3.6 Comparison of the foundation input motion (E/b_e is set as a parameter. c/b=1)

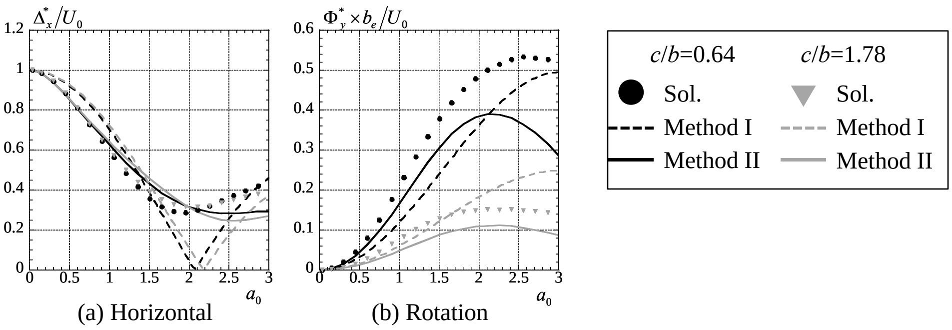

Figure 3.7 Comparison of the foundation input motion (c/b is set as a parameter. E/b_e=1)

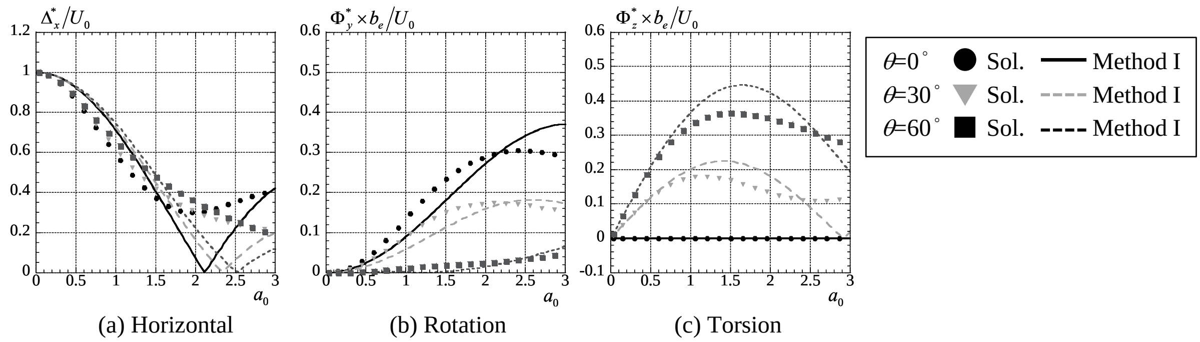

Figure 3.8 Comparison of the foundation input motion of each component (c/b=1、E/b_e=1)

Next, the foundation input motions obtained by two simplified methods are compared to the theoretical solution. For the case of that the ratio of the depth to the equivalent width E/b_e is set as a parameter, Fig. 3.6 compares the embedded foundation input motions using the proposed simplified methods I, II with those obtained by the theoretical solution. Fig. 3.7 shows the same as Fig. 3.6 for the case of that the aspect ratio of the foundation shape c/b is set as a parameter. Fig. 3.8 compares the embedded foundation input motions using the proposed simplified method I with those obtained by the theoretical solution when the incident angle of SH wave is set as a parameter. The foundation input motions in (a) horizontal and (c) torsional components calculated by the proposed simplified method I are found to be zero at some frequency as shown in Figs. 3.6 to 3.8. It is because that the solutions of Eqns. 2.15 to 2.19 are real numbers or pure imaginary numbers and that the method is very simple way without the impedance. It is found in Fig. 3.6 that (a) horizontal component obtained by the simplified method II is good correspondence with the theoretical solution. Furthermore, as for (b) rotational component, the peak frequency calculated by the simplified method I is higher than that of the theoretical solution and the amplitude at this point is overestimated, and the simplified method II can explain the tendency of the foundation input motion approximately. Fig. 3.7 indicates that the proposed simplified methods I and II can grasp roughly the tendency of the foundation input motion depending on the aspect ratio of the foundation shape.

From Fig. 3.8, we find some characteristics of the proposed methods as follows:

(1) The proposed simplified methods I (Method I) can explain approximately the second peak of the theoretical solution though the foundation input motion becomes zero at a frequency.
(2) As for (b) rotation and (c) torsional component, the amplitude at the peak frequency is overestimated as shown in Fig. 3.6, and the tendency that the rotational response decreases and torsional response increases according to the increasing of the incident angle of SH wave is able to be presented sufficiently.

It is concluded that the proposed method II (Method II) is the practical method and that the proposed method I (Method I) can explain roughly the tendency of the foundation input motion.

4. CONCLUSIONS

It this study, we proposed new two conventional evaluation methods of the foundation input motion. The simplified method I is to calculate the input motion by using the geometrical relationship between the embedded foundation and the input ground motion. The simplified method II is to calculate it by using the driving force which is obtained from the input ground motion and the impedance of the embedded foundation. The impedance of the embedded foundation is derived from that of the spread foundation corrected using the conventional modification functions proposed in this study. Both proposed methods obtain the results which have good agreement with the theoretical solutions. The simplified method I is useful for the first stage of the structure design to grasp the dynamic characteristics of the building because the solution is presented in the explicit function. The simplified method II will be able to apply to problems under various conditions because of its high accuracy.

REFERENCES

AIJ (2010). An introduction to dynamic soil-structure interaction, the Architectural Institute of Japan (in Japanese).

K. Sugimoto *et al.* (2010): Building Seismic Response Analysis Model Considering Coupling Behaviour of the Base Mat due to Uplift in a Vibrating Direction, *Summaries of technical papers of Annual Meeting Architectural Institute of Japan. B-2,* **Structures II:** pp.683-684 (in Japanses).

M. Iguchi (1982). An Approximate Analysis of Input Motions for Rigid Embedded Foundations, *Transactions of the Architectural Institute of Japan*, **No.315:** pp.61-75.

M. Mori *et al.* (2008). Effects of Side and Base Elements of Embedded Spread Foundations on Dynamic Soil-Structure Interaction and Conventional Estimation Methods for Soil Springs by Composing the Impedance of Each Element, *Journal of structural and construction engineering. Transactions of AIJ,* **No.626:** pp.535-542 (in Japanese).

O. Kurimoto and M. Iguchi (1995). Evaluation of Foundation Input Motions Based on Observed Seismic Waves, *Journal of structural and construction engineering. Transactions of AIJ,* **No.472:** pp.67-74 (in Japanese).

O. Kurimoto and T. Seki (1995). A Simple Method for Evaluating Dynamic Characteristics of Partially Embedded Foundation, *Journal of structural and construction engineering. Transactions of AIJ,* **No.486:** pp.19-26 (in Japanese).

X. Wen and N. Fukuwa (2006). The Effects of Adjacent Building on Soil-Structure Interaction, *Journal of structural and construction engineering. Transactions of AIJ,* **No.600:** pp.97-105 (in Japanese).